

Detecting and imaging single Rydberg electrons in a Bose-Einstein condensate

Tomasz Karpiuk,^{1,2} Mirosław Brewczyk,^{1,3} and Kazimierz Rzażewski^{3,4}

¹*Wydział Fizyki, Uniwersytet w Białymstoku, ul. Lipowa 41, 15-424 Białystok, Poland*

²*Centre for Quantum Technologies, National University of Singapore, 3 Science Drive 2, Singapore 117543, Singapore*

³*Center for Theoretical Physics PAN, Al. Lotników 32/46, 02-668 Warsaw, Poland*

Jonathan B. Balewski⁴, Alexander T. Krupp⁴, Anita Gaj⁴, Robert Löw⁴, Sebastian Hofferberth⁴ and Tilman Pfau⁴

⁴*Physikalisches Institut, Universität Stuttgart, Pfaffenwaldring 57, 70569 Stuttgart, Germany*

The quantum mechanical states of electrons in atoms and molecules are discrete spatial orbitals, which are fundamental for our understanding of atoms, molecules, and solids. They determine a wide range of basic atomic properties, ranging from the coupling to external fields to the whole field of chemistry. Nevertheless, the manifestation of electron orbitals in experiments so far has been rather indirect. In a detailed theoretical model, we analyze the impact of a single Rydberg electron onto a Bose-Einstein condensate and compare the results to experimental data. Based on this validated model we propose a method to optically image the shape of single electron orbitals using electron-phonon coupling in a Bose-Einstein condensate. This scheme requires only established and readily available experimental techniques and allows to directly capture textbook-like spatial images of single electronic orbitals in a single shot experiment.

Electron orbitals form the basis of our understanding of atoms, molecules, and solids. The electromagnetic interaction of an atom with its surrounding is dominated by these orbitals, determining e.g. optical and chemical properties of matter. Despite their large impact on all these different aspects, the direct imaging of electronic orbitals is a challenging task. Most techniques to study the wavefunction of electrons in atoms and molecules rely on tomographic reconstruction. The wavefunction of the highest occupied molecular orbital of different molecules has been reconstructed using high harmonics generated from intense femtosecond laser pulses [1] and photoemission spectroscopy [2]. Another method, which has been so far mostly applied to larger polymers, is based on scanning tunneling microscopy [3–5]. A different approach has been realized recently to study the electron wavefunction in single hydrogen atoms [6]. In this work, peculiar electronic states in a strong static electric field, so called Stark states, were directly imaged via photoionization and subsequent electron detection using a magnifying electrostatic lens. However, a direct spatial mapping of single spatial atomic orbitals, as known from basic quantum theory, has been elusive so far.

In order to investigate single electron orbitals with purely optical methods, highly excited Rydberg states with principal quantum number n above ~ 100 provide orbitals with sizes larger than the optical wavelength, i.e. the resolution limit of optical microscopy. These orbitals can be very well controlled in all their quantum numbers and provide for example clean s, p, d, and f series. Even more interesting orbitals for single electrons in electric and magnetic fields or after a pulsed sequence of electric fields include circular Rydberg states [7], Stark states, Bohr-like wavepackets [8, 9], and one dimensional atoms [10]. Furthermore, this approach can also be extended to more complex systems like Rydberg-atom macrodimers [11].

Here, we propose a new method to optically image the orbitals of high Rydberg states in a Bose-Einstein condensate.

The interaction of the dense ultracold gas with the Rydberg electron [12] imprints the probability density of a single Rydberg electron as a density modulation onto the BEC. As a consequence, using well-established imaging techniques for cold atoms, textbook-like optical images of hydrogenic states can be obtained. First we study the interaction of a series of individual Rydberg atoms with the condensate and compare the results with experimental data. Then we apply our theoretical model to propose a method to directly observe the imprint of the electronic orbital on the density distribution of the condensate.

In our recent experiment [12], a single Rydberg atom in an s-state with principal quantum numbers n ranging from 110 to 202 was created in a ^{87}Rb condensate of around $N = 80000$ atoms. Its radius, scaling with $\sim n^2$, varies from 1 to $4\mu\text{m}$, and is thus clearly within the resolution of optical imaging techniques. Furthermore, highly excited Rydberg atoms interact strongly via induced dipole-dipole forces. As a result, the Rydberg blockade [13] allows only a single Rydberg excitation at a time within the volume of the BEC in [12]. The single electron of a Rydberg atom polarizes near-by atoms. The interaction potential, falling-off with a distance like $1/r^4$, is of short range type. Hence a pseudopotential [14, 15] may be used to approximately describe the interaction energy between the electron and the surrounding ground state atoms:

$$V_{\text{Ryd}}(\vec{r}) = \frac{2\pi\hbar^2 a}{m_e} |\Psi_{\text{Ryd}}(\vec{r})|^2, \quad (1)$$

where $\Psi_{\text{Ryd}}(\vec{r})$ is the Rydberg electron wavefunction, a denotes the electron-atom s-wave scattering length and m_e is the electron mass, to a good approximation the reduced mass of atom-electron system. The triplet scattering length of the electron-atom interaction relevant here is $a = -16.1$ in units of the Bohr radius [16]. Note that the corresponding interaction energy of the positive ion of the Rydberg atom has a reduced mass next to five orders of magnitude larger, so that its impact on the condensate can be neglected. In the range

of n from 110 to 202, between 700 and 20000 ground state atoms are located inside the classically allowed region of the Rydberg electron in our experiment. The interaction of the Rydberg electron with these atoms adds up to a mean energy shift, which is only depending on the atomic density $\rho(\vec{r})$ and the electron-atom scattering length [14, 17]:

$$\delta E(\vec{R}) = \int V_{Ryd}(\vec{r} - \vec{R}) \rho(\vec{r}) d^3 r. \quad (2)$$

This shift depends on the position \vec{R} of the Rydberg atom in the condensate. To describe the effect of the Rydberg electron on the condensate, the pseudopotential (1) is introduced as an additional term in the Gross-Pitaevskii equation describing the dynamics of the bosonic atomic field. We adopt a classical field approximation, where a long-wavelength atomic field is stripped off its operator character and is replaced by a classical, complex function $\Psi(\vec{r}, t)$ satisfying the time-dependent equation:

$$i\hbar \frac{\partial}{\partial t} \Psi(\vec{r}, t) = \left[-\frac{\hbar^2}{2m} \nabla^2 + V_{trap}(\vec{r}) + g|\Psi(\vec{r}, t)|^2 + f(t) V_{Ryd}(\vec{r} - \vec{R}) \right] \Psi(\vec{r}, t). \quad (3)$$

In the right-hand side, the usual terms related to the kinetic energy, the trapping potential, and the contact interaction with coupling constant g appear. The pseudopotential term is multiplied by a function $f(t)$ which takes the values 0 or 1, depending on whether a Rydberg atom is present, centered at position \vec{R} . The interaction is present only during the lifetime of the Rydberg atom within a single creation cycle.

The results in [12] were obtained by repeating $1\mu s$ long Rydberg excitation pulses 300 – 500 times. Thus it is crucial to appropriately model the excitation process in order to reproduce the experimental findings. For sufficiently short times t and low single atom Rabi frequencies Ω_R , the probability to find an atom at position \vec{R} in the Rydberg state is given as

$$p(\vec{R}, t) = \frac{\Omega_R^2}{\Omega^2(\vec{R}, t)} \sin^2 \left[\Omega(\vec{R}, t) t / 2 \right], \quad (4)$$

where the effective Rabi frequency $\Omega(\vec{R}, t)$ takes a non-zero local detuning $\Delta(\vec{R}, t)$ into account:

$$\Omega(\vec{R}, t) = \sqrt{\Omega_R^2 + \Delta^2(\vec{R}, t)}. \quad (5)$$

The resonant Rabi frequency Ω_R is the single atom Rabi frequency. For the experiment of Ref. [12] these frequencies are estimated to vary in the range of a few kHz. The spatially dependent detuning $\Delta(\vec{R}, t)$ accounts for the laser detuning $\Delta\omega_L$ from the vacuum Rydberg level and the density dependent shift of the Rydberg level $\delta E(\vec{R}, t)$, given by equation (2):

$$\Delta(\vec{R}, t) = \Delta\omega_L - \delta E(\vec{R}, t) / \hbar \quad (6)$$

Since the condensate density changes due to disturbance caused by the appearance of successive Rydberg atoms, the

detuning Δ and thus the excitation probability (4) depend also on time.

So far, equation (4) does neither fully take the interaction of the Rydberg electron with the dense atomic sample nor the Rydberg blockade into account. The coupling of the Rydberg electron to the condensate causes a process which identifies (i.e. measures) the position of the Rydberg atom, projecting the system on the basis of single localized Rydberg excitations. At this point, the coherent evolution of the excitation, described by equation (4), stops. We assume that this process originates from the elastic scattering of the Rydberg electron at the atoms in the condensate. In a semiclassical picture, the scattering rate is on the order of some MHz. In order to account for both the Rydberg blockade and this process, we interrogate the system every 200ns, a rough estimate for the duration between two scattering events. To determine if and where a Rydberg atom is excited, we then use the following procedure: First, we choose a position of a possible excitation according to the density distribution $\rho(\vec{r})$. According to the excitation probability (4) we draw a random number to determine if an excitation indeed takes place. If yes, $f(t)$ changes its value from 0 to 1 and the time evolution of the BEC continues governed by equation (3). If not, another position is picked randomly and the procedure is repeated until either an excitation occurs or the number of trials reaches 80000, the total number of atoms. In the latter case, no Rydberg excitation occurs during this time step and we advance by a time-step of 200ns, repeating the stochastic procedure until the end of excitation pulse of $1\mu s$. Once created, the interaction of the Rydberg electron with the condensate is limited by the experimental sequence length of 10 microseconds and the decay of the Rydberg state. Based on the measurements in [12], we assume a mean lifetime of 10 microseconds for all Rydberg states. A cycle consisting of the excitation of the Rydberg atom followed by a finite interaction time with the condensate atoms is repeated 300 or 500 times.

Heated by the time-dependent potential, the condensate undergoes losses. Some atoms are promoted to the thermal cloud. These losses were measured in [12]. Within the classical field approximation the two components of the bosonic gas – the condensate and the thermal cloud are identified by accounting for the coarse graining as an unavoidable element of the measurement process [18]. In the case of a nontrivial dynamics, in tune with the actual imaging method, we define a coarse grained one-particle density matrix as resulting from the column integration [19]:

$$\bar{\rho}(x, z, x', z'; t) = \frac{1}{N} \int dy \Psi(x, y, z, t) \Psi^*(x', y, z', t). \quad (7)$$

Here we adopt imaging performed along the radial direction (condensate symmetry axis is the z axis). The resulting density matrix, upon spectral decomposition [20], determines the fraction of the condensed atoms as a dominant eigenvalue. For a direct comparison with the experiment we calculate the total condensate losses at the end of the excitation sequence and

divide them by the number of excitation cycles. We study the dependence of this quantity as a function of the laser detuning $\Delta\omega_L$ and the principal quantum number n of the Rydberg state. In Fig. 1 (top frame) we show the laser detuning

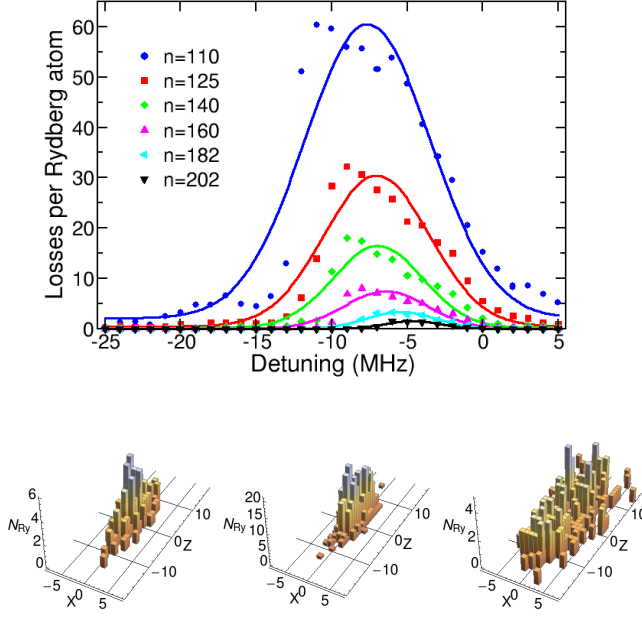


FIG. 1. (color online). Theoretically calculated losses of atoms from the condensate per Rydberg atom excitation versus the detuning from the non-interacting Rydberg level (top frame). Solid lines are Gaussian fits. Bottom panel: A single realization real-space distribution of Rydberg atoms for $n = 110$ and $\Delta\omega_L = -13$ MHz (left frame), -9 MHz (middle frame), and 1 MHz (right frame).

dependent losses for various Rydberg states. Away from the spectral position of maximal losses, more pulses create no Rydberg atoms. On the right-hand side of the resonance losses are small because Rydberg atoms are excited almost homogeneously in space as it is visible in the right histogram of Fig. 1 (bottom frame). So, many excitations are created in regions of low density, leading to reduced losses. Towards the center of the line more Rydberg atoms are created around the center of the trap where the density of the condensate is high. This leads to the increase of losses reaching their maximum approximately where $\Delta\omega_L$ is equal to $\delta E(\vec{R}, t)/\hbar$ calculated at the center of the trap. The distribution of Rydberg atoms for the center of the line is shown in the middle histogram of Fig. 1. On the left-hand side of the resonance the situation is different. Still many Rydberg atoms are created in the center of the trap (see left histogram of Fig. 1). However, Rydberg atoms are not created in every excitation cycle and thus the overall losses decrease. On the blue side of the resonance, a Rydberg atom is created almost at every shot. To the red of the resonance, fewer Rydberg atoms are excited. In the case of $n = 110$ and $\Delta\omega_L = -12$ MHz for example, roughly every two third excitation pulses creates a Rydberg excitation while

only every seventh trial is successful at $\Delta\omega_L = -16$ MHz. The absolute values of maximal losses as computed from the

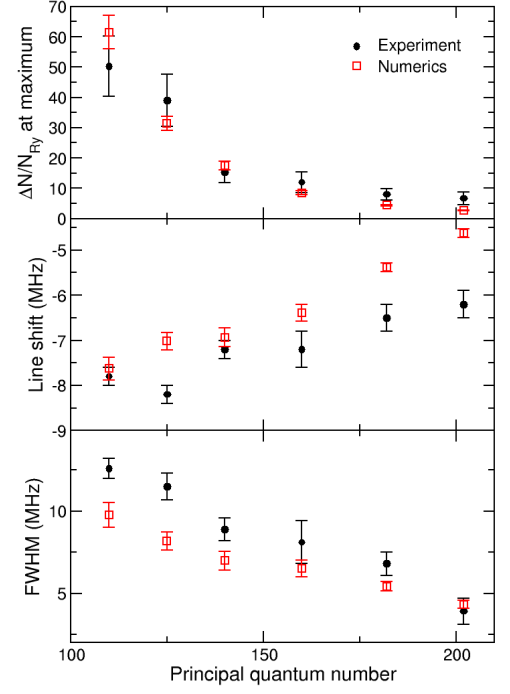


FIG. 2. (color online). Comparison between theoretical (red open squares) and experimental (black dots) results. Theoretical results have been obtained from Gaussian fits to numerical data shown in Fig. 1. The frames depict (from top to bottom) the maximum losses of atoms from the condensate per Rydberg excitation, the position of the resonance, and the FWHM of the resonance lines.

Gaussian fits to our numerical data from Fig. 1 are compared to the experimental data from [12] in Fig. 2 (top frame). We extract also the position of the resonance (middle frame) and the width of the line (bottom frame) from the fits. The error bars are the statistical errors resulting from the Gaussian fits. The numerical results agree remarkably well with the experimental data considering the fact that estimated values of the Rabi frequencies and no additional free parameters were used. Having demonstrated the validity of our theoretical model, we now turn to the proposal of observing an electronic orbital by imaging the response of the condensate density to the potential (1). We assume a tightly focused excitation laser in order to spatially define the position of the Rydberg atom at the center of the condensate. Rydberg s - and d -states accessible in typical two-photon excitation schemes [21, 22] are considered. First we study a single Rydberg excitation, present in the condensate during a lifetime of $10\mu s$. A contrast of few percent is achieved in the density patterns $90\mu s$ after the Rydberg atom has decayed (right panels of Fig. 3). In this case relatively low principal quantum numbers are favorable because their potential wells are deeper. A larger effect, also at higher principal quantum numbers, can be obtained if the process of

Rydberg excitation is repeated multiple times as in Ref. [12]. We assume here that the blue laser beam is focused in such a way that the intensity of light in the center of a condensate is Gaussian with the diameter (at $1/e^2$ of magnitude) equal to $1.2\mu\text{m}$. A good trade-off between sufficient contrast in the density profile and a reasonable sharpness of the image is then obtained for around 50 excitation cycles (see movies available at [23]).

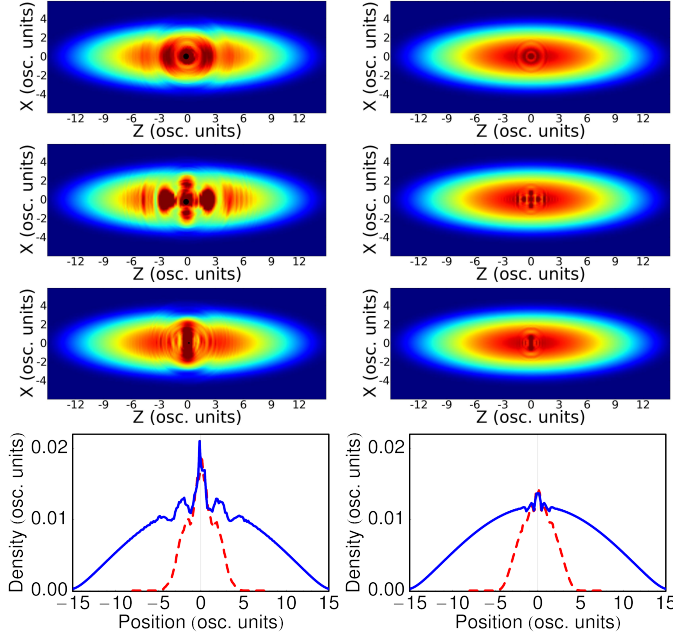


FIG. 3. (color online). Left panels: Density distribution of the Bose-Einstein condensate after 50 Rydberg atoms have been excited. The black dot around the middle of the trap indicates the center position of the last Rydberg atom. The panels correspond to excitations of different Rydberg atom states (from the top to bottom): $|n = 182, l = 0, m_l = 0\rangle$, $|n = 180, l = 2, m_l = 0\rangle$, and $|n = 180, l = 2, m_l = 2\rangle$. The condensate consisting initially of 8×10^4 rubidium atoms is confined in a harmonic trap with radial and axial frequencies $\omega_r = 2\pi \times 81.7\text{ Hz}$ and $\omega_z = 2\pi \times 22.4\text{ Hz}$, respectively. The oscillatory unit of length is defined via the radial trap frequency, $\sqrt{\hbar/m\omega_r}$, and equals $1.19\mu\text{m}$. The right panels: Density patterns after exciting just a single Rydberg atom at the center of the trap for the duration of $10\mu\text{s}$, after an additional delay time of $90\mu\text{s}$. Here, from the top to bottom the Rydberg state is: $|n = 110, l = 0, m_l = 0\rangle$, $|n = 106, l = 2, m_l = 0\rangle$, and $|n = 106, l = 2, m_l = 2\rangle$. See also movies available at [23]. Lowest frames: Axial (solid blue lines) and radial (dashed red lines) density cuts for $|n = 182, l = 0, m_l = 0\rangle$ (after exciting 50 Rydberg atoms, left) and $|n = 110, l = 0, m_l = 0\rangle$ (after exciting just a single Rydberg atom, right) states.

To summarize: We have presented the first full theoretical, microscopic model of a single Rydberg atom electron in a Bose-Einstein condensate. Good agreement with the available results for the s -state Rydberg atoms is demonstrated. We also propose a novel scheme for mapping the electronic orbital on the density of the condensate realizing a method to directly observe the various electronic orbitals. The technical requirements with respect to resolution, both for the local

excitation of Rydberg atoms and the detection of the resulting structures, are met by state of the art experimental setups. Furthermore, various techniques like dark ground imaging [24], phase-contrast imaging [25], polarization contrast imaging [26, 27], and adapted forms of absorption imaging [28] are readily available to precisely determine the density distribution of a BEC in situ. The optical imaging of a single electron in a single shot experiment seems thus in direct reach.

Acknowledgments: We are grateful to Mariusz Gajda and Tomasz Sowiński for helpful discussions. The work was supported by the National Science Center grants No. DEC-2011/01/B/ST2/05125 (T.K.) and DEC-2012/04/A/ST2/00090 (M.B., K.R.). K.R. acknowledges the financial support from the project “Decoherence in long range interacting quantum systems and devices” supported by contract research “Internationale Spitzenforschung II” of the Baden-Württemberg Stiftung. The CQT is a Research Centre of Excellence funded by the Ministry of Education and the National Research Foundation of Singapore. The experimental work is funded by the Deutsche Forschungsgemeinschaft (DFG) within the SFB/TRR21 and the project PF 381/4-2. We also acknowledge support by the ERC under contract number 267100 and from E.U. Marie Curie program ITN-Coherence 265031. S.H. is supported by the DFG through project HO 4787/1-1.

-
- [1] J. Itatani, J. Levesque, D. Zeidler, H. Niikura, H. Pepin, J. C. Kieffer, P. B. Corkum, and D. M. Villeneuve, *Nature* **432**, 867 (2004).
 - [2] P. Puschnig, S. Berkebille, A. J. Fleming, G. Koller, K. Emtsev, T. Seyller, J. D. Riley, C. Ambrosch-Draxl, F. P. Netzer, and M. G. Ramsey, *Science* **326**, 702 (2009).
 - [3] J. Repp, G. Meyer, S. M. Stojković, A. Gourdon, and C. Joachim, *Phys. Rev. Lett.* **94**, 026803 (2005).
 - [4] L. Gross, N. Moll, F. Mohn, A. Curioni, G. Meyer, F. Hanke, and M. Persson, *Phys. Rev. Lett.* **107**, 086101 (2011).
 - [5] Z. Cheng, S. Du, W. Guo, L. Gao, Z. Deng, N. Jiang, H. Guo, H. Tang, and H.-J. Gao, *Nano Research* **4**, 523 (2011).
 - [6] A. S. Stodolna, A. Rouzée, F. Lépine, S. Cohen, F. Robicheaux, A. Gijsbertsen, J. H. Jungmann, C. Bordas, and M. J. J. Vrakking, *Phys. Rev. Lett.* **110**, 213001 (2013).
 - [7] R. G. Hulet and D. Kleppner, *Phys. Rev. Lett.* **51**, 1430 (1983).
 - [8] J. J. Mestayer, B. Wyker, J. C. Lancaster, F. B. Dunning, C. O. Reinhold, S. Yoshida, and J. Burgdörfer, *Phys. Rev. Lett.* **100**, 243004 (2008).
 - [9] H. Maeda, J. H. Gurian, and T. F. Gallagher, *Phys. Rev. Lett.* **102**, 103001 (2009).
 - [10] M. Hiller, S. Yoshida, J. Burgdörfer, S. Ye, X. Zhang, and F. B. Dunning, *Phys. Rev. A* (2014), accepted.
 - [11] K. R. Overstreet, A. Schwettmann, J. Tallant, D. Booth, and J. P. Shaffer, *Nature Physics* **5**, 581 (2009).
 - [12] J. B. Balewski, A. T. Krupp, A. Gaj, D. Peter, H. P. Büchler, R. Löw, S. Hofferberth, and T. Pfau, *Nature* **502**, 664 (2013).
 - [13] M. Saffman, T. G. Walker, and K. Mølmer, *Rev. Mod. Phys.* **82**, 2313 (2010).
 - [14] E. Fermi, *Nuovo Cimento* **11**, 157 (1934).
 - [15] E. Fermi, *Ric. Scientifica* **7**, 13 (1936), translated by G. M. Tem-

- mer in Enrico Fermi, *Collected Papers Volume I*, university of Chicago press, 1962.
- [16] C. Bahrim, U. Thumm, and I. I. Fabrikant, J. Phys. B: At. Mol. Opt. Phys. **34**, L195 (2001).
 - [17] E. Amaldi and E. Segrè, Nature **133**, 141 (1934).
 - [18] K. Góral, M. Gajda, and K. Rzazewski, Opt. Express **8**, 92 (2001).
 - [19] T. Karpiuk, M. Brewczyk, M. Gajda, and K. Rzazewski, Phys. Rev. A **81**, 013629 (2010).
 - [20] O. Penrose and L. Onsager, Phys. Rev. **104**, 576 (1956).
 - [21] R. Löw, H. Weimer, J. Nipper, J. B. Balewski, B. Butscher, H. P. Büchler, and T. Pfau, J. Phys. B: At. Mol. Opt. Phys. **45**, 113001 (2012).
 - [22] M. Viteau, J. Radogostowicz, M. G. Bason, D. Malossi, N. Ciampini, O. Morsch, and E. Arimondo, Opt. Express **19**, 6007 (2011).
 - [23] alpha.uwb.edu.pl/brewczyk.
 - [24] M. R. Andrews, M.-O. Mewes, N. J. van Druten, D. S. Durfee, D. M. Kurn, and W. Ketterle, Science **273**, 84 (1996).
 - [25] M. R. Andrews, D. M. Kurn, H.-J. Miesner, D. S. Durfee, C. G. Townsend, S. Inouye, and W. Ketterle, Phys. Rev. Lett. **79**, 553 (1997).
 - [26] C. C. Bradley, C. A. Sackett, and R. G. Hulet, Phys. Rev. Lett. **78**, 985 (1997).
 - [27] F. Kaminski, N. Kampel, M. Steenstrup, A. Griesmaier, E. Polzik, and J. Müller, EPJ D **66**, 1 (2012).
 - [28] G. E. Marti, R. Olf, and D. M. Stamper-Kurn, arXiv:1210.0033 (2012), arXiv:1210.0033 [cond-mat.quant-gas].